Interactions between Fatty Acids and Lipoprotein Lipase: Specific Binding and Complex Formation†

K. Edwards,*,‡ R. Y. S. Chan,§ and W. H. Sawyer§

The Russell Grimwade School of Biochemistry, University of Melbourne, Parkville, Victoria 3052, Australia, and the Department of Physical Chemistry, Uppsala University, Box 532, S-751 21 Uppsala, Sweden

Received June 6, 1994; Revised Manuscript Received August 19, 1994⊗

ABSTRACT: Lipoprotein lipase is the extrahepatic lipase responsible for the hydrolysis of triglycerides in chylomicrons and very low-density lipoproteins. Its enzymic activity and its location on the surface of endothelial cells are affected by the presence of fatty acids, implying that the protein possesses binding sites for that ligand. In this study, we examine the binding of fatty acids to LpL and describe factors that must be considered when the dissociation constant of the acceptor−ligand equilibrium is close to the critical micelle concentration of the fatty acid. The interaction of fatty acids with lipoprotein lipase (LpL) was studied by two methods. A new direct method, based on the LpL-induced increase in the apparent critical micelle concentration of the sodium soap of the fatty acid, indicates the presence of multiple high-affinity binding sites. In the second method, the specific binding of fatty acids to LpL was measured by quantitating the blue shift in the tryptophan fluorescence of LpL that occurs upon binding the ligand. Both methods suggest the existence of 4−6 fatty acid binding sites on LpL with a dissociation constant on the order of 10^{-6}−10^{-7} M. Further analysis of the blue shift indicates that at higher concentrations of fatty acid, large complexes are formed consisting of 260−310 molecules of fatty acid per LPL monomer. In contrast, no large complexes are formed with fatty acids that form crystals above their solubility limit.

Lipoprotein lipase (LpL[1]) is the extrahepatic lipase responsible for the hydrolysis of triglycerides to glycerol and fatty acids. The enzyme is bound to heparin-like glycosaminoglycans at the luminal surface of endothelial cells and acts primarily on triglycerides in chylomicrons and very low-density lipoproteins (VLDL). Several studies indicate that the fatty acid products of lipolysis regulate both LpL activity and the in vivo location of the enzyme. In vitro studies have shown that fatty acids dissociate LpL bound to heparin−Sepharose (Olivecrona & Bengtsson-Olivecrona, 1985) and heparin−agarose (Peterson et al., 1990). At another level, it has been shown that fatty acids release LpL from the endothelial cell wall (Saxena et al., 1989). These experiments indicate that fatty acids can interact with the heparin−LpL complex. However, release of LpL from the cell wall does not completely account for the effects of fatty acids. In a phospholipid-stabilized triglyceride emulsion, the production of fatty acids by lipolysis inhibits the enzyme. Maximum rates are not attained unless fatty acids are removed by the inclusion of bovine serum albumin in the mixture (Bengtsson & Olivecrona, 1980; Posner & DeSanctis, 1987). Addition of oleic acid in the absence of serum albumin inhibits lipolysis. Part of this effect may be attributed to the ability of fatty acids to inhibit the binding of LpL to apolipoprotein C-II, the protein that normally enhances LpL activity (Bengtsson & Olivecrona, 1979). On the other hand, kinetic analyses indicate that oleic acid competes with triglyceride for the active site of the enzyme and that LpL may possess approximately four binding sites for oleic acid per monomer (Posner & DeSanctis, 1987). However, no direct measurements of the binding of fatty acids to LpL have been reported. Apart from the inhibition of enzymic activity, fatty acids are known to stabilize LpL in solution and to prevent its precipitation in low ionic strength buffers. This effect, which is also observed with other surfactants (Baginsky & Brown, 1977), is believed to be due to the adsorption of LpL to a lipid surface, whether it be a micelle, emulsion, or phospholipid bilayer. Little is known of the nature of these complexes, although recent X-ray diffraction data for pancreatic lipase suggest that binding to a lipid surface results in a conformational change that involves the lifting of a cap that normally obscures the active site of the enzyme (van Tilbeurgh et al., 1993); homology modeling predicts that a similar cap exists in the case of LpL (van Tilbeurgh et al., 1994).

At a more general level, intracellular and extracellular transport of fatty acids is mediated by fatty acid binding proteins, many of which have been purified and characterized. The binding characteristics of these proteins have been studied using a variety of techniques—equilibrium dialysis, the partition of fatty acid between the heptane and water−albumin phases, ESR, and NMR—and using spectroscopic techniques employing fluorescent fatty acids or a fluorescently tagged fatty acid binding protein [Richieri et al., 1992; for a review see Spector (1986)]. In many cases the dissociation constants fall in the region where fatty acids are known to form micelles. The difficulty that micelle

† This work was supported by the National Heart Foundation of Australia. K.E. was financially supported by the Swedish Natural Science Research Council and the Swedish Institute. K.E. was a visiting Postdoctoral Fellow at The Russell Grimwade School of Biochemistry, University of Melbourne.

* Corresponding author.
‡ Uppsala University.
§ University of Melbourne.

⊗ Abstract published in *Advance ACS Abstracts,* October 15, 1994.

[1] Abbreviations: LpL, lipoprotein lipase; FA, fatty acid(s); VLDL, very low-density lipoprotein(s); SDS, sodium dodecyl sulfate; CMC, critical micelle concentration.

0006-2960/94/0433-13304$04.50/0

formation creates in the conduct of these experiments and in the formulation of any binding model is rarely acknowledged. Thus, a secondary aim of this study is to examine the interplay between micelle formation and the acceptor–ligand equilibrium. Our approach has been to make use of micelle formation itself to examine the binding equilibrium.

MATERIALS AND METHODS

Chemicals and the Preparation of LpL. Fatty acids were purchased from Nu-Chek-Prep Inc. (Elysian, MN) and used without further purification. Concentrated stock solutions were prepared by dissolving the fatty acids in ethanol. LpL was isolated from bovine skim milk and purified on an affinity column of heparin–agarose gel, as described by McLean and Jackson (1985) and Bengtsson-Olivecrona and Olivecrona (1990). The standard buffer used in all experiments contained 10 mM Tris-HCl, 1.5 M NaCl, 1 mM EDTA, and 0.01% NaN_3 (pH 7.4). The high concentration of NaCl was required to prevent aggregation and subsequent precipitation of the LpL.

Determination of the Apparent Critical Micelle Concentration of the Fatty Acid. Small aliquots of the concentrated stock solution of fatty acid were added to a thermostated (25 °C) quartz cuvette containing 2.6 mL of buffer and the desired amount of LpL. The total volume of added stock solution never exceeded 26 μl. The cell was placed in a Perkin-Elmer LS5 spectrofluorometer with both the excitation and emission monochromators set at 400 nm. After each addition, the sample was allowed to equilibrate for 2 min before the intensity of scattered light at 90° to the incident beam was measured. The apparent critical micelle concentration was taken as the fatty acid concentration at which the intensity of scattered light began to increase sharply in a linear fashion. All aqueous stock solutions were passed through 0.45 μm filters to remove particulate material.

Intrinsic LpL Fluorescence. LpL undergoes a small blue shift in intrinsic fluorescence upon binding fatty acids. To titrate this change, aliquots of fatty acid were added to a cuvette containing LpL in standard buffer. After equilibration for 2 min, the emission spectrum was recorded using a Perkin-Elmer LS5 spectrofluorometer. The excitation wavelength was 280 nm. Because of the broadness of the emission band and the difficulty of accurately determining the emission maximum, the spectral change was also quantitated by determining the change in the ratio of emission intensities at 318 and 342 nm relative to that for LpL in the absence of ligand. The shift in the ratio was then plotted against the concentration of fatty acid. In these experiments, the temperature was kept at either 20 or 25 °C.

RESULTS

CMC Measurements of Fatty Acids. Fatty acids can form micelles at temperatures above their melting temperature. At the CMC, abrupt changes occur in several physical properties of the fatty acid solution (surface tension, osmotic pressure, conductance, light scattering) and these may be used to determine the concentration at which micelles begin to form. Figure 1 shows a plot of 90° light scattering as a function of oleate concentration.[2] After an initial shallow increase at low concentrations, the scattered intensity increases sharply and linearly due to the formation of micelles. The intersection of the two linear parts of the plot is a good approximation of the CMC. At high fatty acid concentrations, the curve begins to deviate from linearity (not shown) probably due to the formation of elongated micellar structures. The CMC for oleate in standard buffer containing 1.5 M NaCl was 1.0 μM (Figure 1). At lower salt concentrations, the net repulsive forces between the negatively charged headgroups increase and the CMC shifts toward higher concentrations. Accordingly, at 0.15 M NaCl, the CMC increased to 6.9 μM. This value is in agreement with the value determined by Richieri et al. (1992) at the same salt concentration.

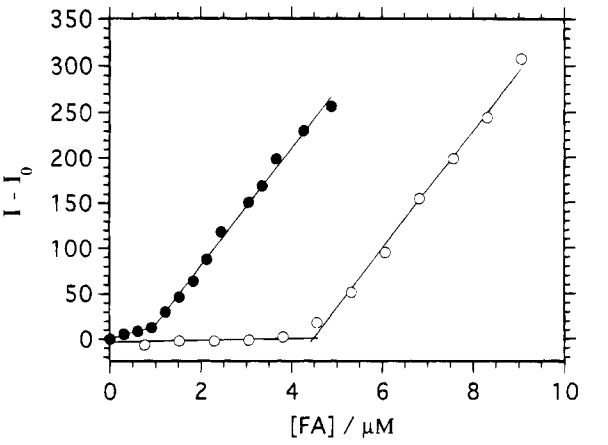

FIGURE 1: Intensity of light scattered at 90° as a function of added oleic acid (●) or linoleic acid (○). The data are presented in terms of the change in intensity relative to a sample of buffer containing no fatty acid. The standard buffer contained 10 mM Tris-HCl, 1.5 M NaCl, 1 mM EDTA, and 0.01% NaN_3 (pH 7.4). The breakpoints at 1.0 and 4.5 μM, respectively, indicate the critical micelle concentrations.

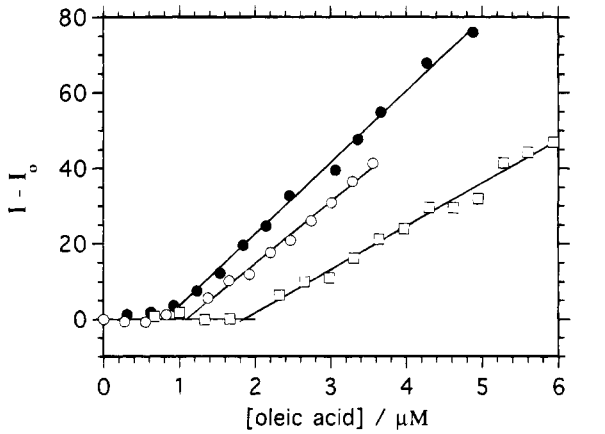

FIGURE 2: Intensity of scattered light as a function of oleic acid concentration in the absence of LpL (●) and in the presence of 0.08 (○) and 0.3 (□) μM LpL. The break points indicate the apparent CMC.

Figure 1 also shows a plot of light scattering as a function of the concentration of linoleic acid. The introduction of a second double bond increases the solubility of the fatty acid soap and shifts the CMC to 4.5 μM in the present buffer system. The difference in the CMC between oleate and linoleate is of the same magnitude as their difference in partitioning between water and heptane: oleic acid is roughly 4 times more soluble in the organic phase than linoleic acid (Simpson et al., 1974).

Measurement of the Apparent CMC To Determine Fatty Acid Binding. Figure 2 shows the intensity of scattered light

[2] At pH 7.4, the added fatty acids will not be completely ionized and the system will contain a mixture of acid and soap (Small, 1986).

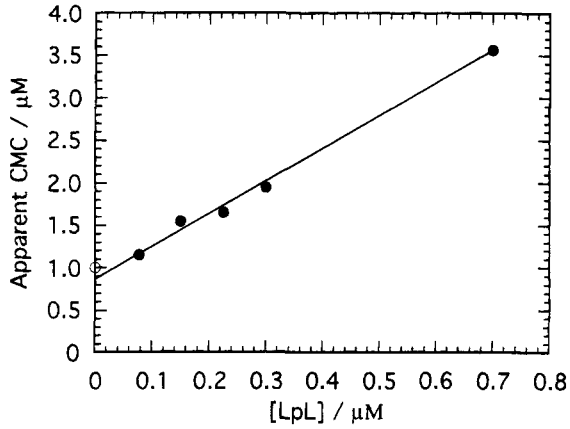

FIGURE 3: Concentration of oleic acid at which the scattered intensity begins to increase plotted as a function of the LpL concentration in accordance with eq 1. The slope (3.8) and intercept (0.86 μM) were obtained by linear regression analysis. The open circle represents the CMC in the absence of LpL.

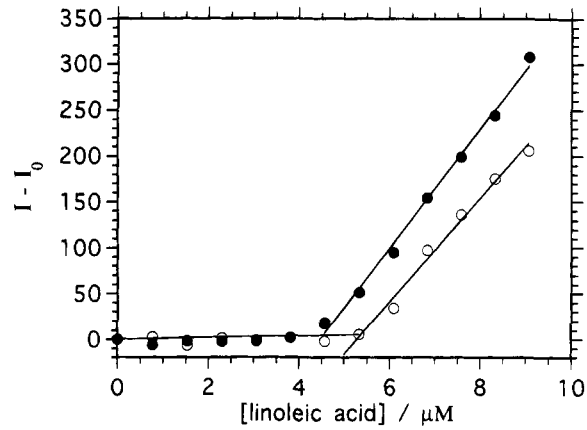

FIGURE 4: Intensity of scattered light as a function of added linoleic acid in the absence (●) and presence (○) of 0.6 μM LpL. The breakpoints occur at 4.5 and 5.4 μM, respectively.

as a function of the concentration of oleic acid for two samples containing different concentrations of LpL. The plots have the same general characteristics as those in the absence of protein, but the steep increase in scattering intensity is moved to higher concentrations of fatty acid. The point where the intensity starts to increase still corresponds to the concentration at which the oleate monomers begin to self-associate to form micellar structures. Thus, provided that the presence of LpL does not influence the formation of micelles, the difference between the apparent CMC (i.e., the total concentration of oleate at which micelles begin to form in the presence of LpL) and the true CMC (determined in the absence of LpL) represents the amount of oleate bound to LpL.

Values of the apparent CMC were determined at a series of LpL concentrations. These data were plotted (Figure 3) according to the linear expression

$$[\text{oleate}]_{\text{tot}} = [\text{oleate}]_{\text{free}} + (([\text{oleate}]_{\text{bound}}/[\text{LpL}]_{\text{tot}})[\text{LpL}]_{\text{tot}}) \quad (1)$$

where $[\text{oleate}]_{\text{tot}}$ and $[\text{oleate}]_{\text{free}}$ are the total and aqueous monomeric concentrations of oleate, respectively, at the point at which self-association begins. Extrapolation to the ordinate intercept provides the CMC in the absence of LpL (0.86 μM). This value is slightly lower than the CMC obtained for oleate in pure buffer (1.0 μM), suggesting that an interaction occurs between the protein and the micellar structures. The decrease in the slope above the apparent CMC with increasing LpL concentration (Figure 2) also suggests that micelles formed in the presence of protein are of a different size or structure than micelles of oleic acid alone. We will return to this question in a later section.

The slope of Figure 3 (3.8) represents the minimum number of fatty acid binding sites on LpL (the actual number could be higher). By assuming four equivalent and independent binding sites, the dissociation constant can be determined through the application of the binding equation:

$$K_d = [\text{oleate}]_{\text{free}}(p([\text{LpL}]_{\text{tot}}/[\text{oleate}]_{\text{bound}}) - 1) \quad (2)$$

where p is the number of binding sites for oleate on each LpL monomer. Equation 2 may be used to calculate K_d values corresponding to any chosen value of p. The assumption that the $p = 4$ and the application of eq 2 to the data in Figure 4 provide a K_d of 0.042 μM for the binding of oleate to LpL. If we assume five or six binding sites for oleate on each LpL monomer, application of eq 2 provides K_d values of 0.27 and 0.49 μM, respectively.

This treatment assumes that equilibrium conditions prevail, that is, that binding sites are not saturated at points where the concentration of free oleate is less than the constitutive CMC (0.86 μM). However, if $K_d \ll$ CMC, saturation of the acceptor will occur before the formation of micelles, and eq 1 converts to

$$[\text{oleate}]_{\text{tot}} = [\text{oleate}]_{\text{free}} + p[\text{LpL}]_{\text{tot}} \quad (3)$$

The slope in Figure 3 then provides the number of binding sites on each LpL monomer. Data analyzed in this way also provide $p = 4$. However, for full saturation of four binding sites to occur when the free concentration of ligand is below 0.86 μM, the dissociation constant must be reduced to unrealistically low values (e.g., $<10^{-8}$ M). It is thus reasonable to suggest that micelle formation occurs before full saturation is reached and that eq 1 therefore holds.

Effect of the Degree of Unsaturation of the Fatty Acid. To determine whether the binding sites on LpL possess any specificity with respect to the nature of the fatty acid, an attempt was made to compare the binding of some saturated and mono- and di-unsaturated fatty acids. Figure 4 shows the scattering intensity as a function of added linoleic acid for a sample containing 0.6 μM LpL. The sodium soap of this di-unsaturated fatty acid has a CMC of 4.5 μM in the present buffer system (Figure 1). The addition of LpL shifts the apparent CMC to higher values. However, the observed shift is significantly smaller than that observed for oleic acid. As shown in Figure 4, an apparent CMC of 5.4 μM is obtained when the sample contains 0.6 μM LpL. By assuming that the difference between the apparent CMC in the presence of LpL and the true CMC obtained in the absence of LpL corresponds to the amount of bound fatty acid, an approximate dissociation constant for the binding of linoleic acid to LpL can be determined by the application of eq 2. For four, five, and six binding sites, respectively, we get K_d values that are about 200, 40, and 28 times higher than those obtained for oleic acid, respectively. If there is an interaction between the self-associated linoleate monomers and the LpL, as is suggested for oleate, the actual K_d values are likely to be somewhat lower. The difference is expected to be small, and the data in Figure 4 thus indicate that the

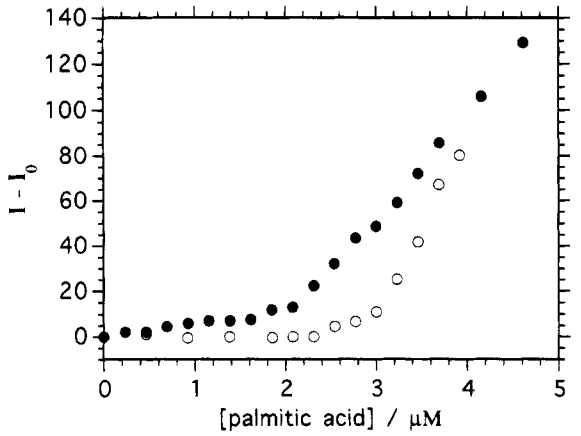

FIGURE 5: Intensity of scattered light as a function of added palmitic acid in the absence (●) and presence of 0.45 μM LpL (○). The observed intensity increases at 4.5 and 5.4 μM fatty acid are due to the formation of acid–soap crystals. Other conditions are as for Figure 1.

addition of a double bond to the acyl chain causes a substantial decrease in the binding affinity. The change is greater than either the difference in CMC or the difference in partition coefficient between the aqueous and organic phases (Simpson et al., 1974). It therefore appears that although the aqueous solubility of the fatty acid monomer is of importance, the conformation of the hydrocarbon chain also influences the binding affinity.

Detection of Crystal Formation by Means of Light Scattering. We now direct attention to the binding of saturated fatty acids to LpL. Palmitic and stearic acids are the most important in a biological context. Both form crystals (rather than micelles) in the current temperature range when the aqueous monomer concentration exceeds the solubility limit. Although the formation of crystals can be readily detected by light scattering measurements, the point at which crystals begin to form is less well defined than in the case of micelle formation (Figure 5). Micelles that form at concentrations just above the CMC are of a well-defined size and homogeneity. In contrast, crystal formation is a slower and more gradual process, with the crystal size increasing as the concentration of solute increases. For the sodium soap of palmitic acid, the scattering intensity starts to increase at concentrations around 2 μM (Figure 5). In this experiment, the temperature (25 °C) was below the melting temperature of the fatty acid, and the increase in scattering is due to the formation of soap, or acid–soap crystals, rather than to micelles. For stearate the solubility limit is too low to be detected by the present method.

We conclude that this method is not well-suited to the detection of subtle changes in the apparent solubility of saturated fatty acids induced by the addition of a fatty acid binding protein.

Intrinsic Fluorescence of LpL. Upon the addition of fatty acids to a solution of LpL, the emission maxima of the intrinsic fluorescence are shifted to lower wavelengths, indicating a more hydrophobic environment of the tryptophan residues. The blue shift is titratable and can be used to quantitatively follow the binding of fatty acids to LpL. For oleic acid, a shift of about 6 nm is observed at full saturation (Figure 6). Because of the broadness of the emission band, the shift can be more accurately quantitated as the ratio of the emission at 318 nm to that at 342 nm, as shown in Figure 6. Figure 7 shows a binding curve obtained upon the

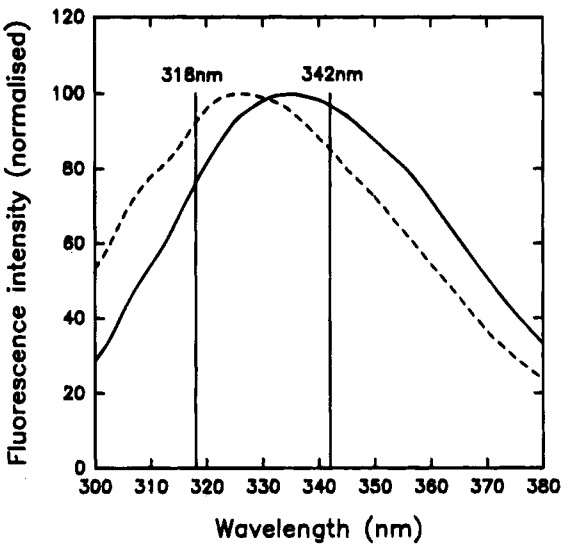

FIGURE 6: Intrinsic fluorescence of LpL (0.15 μM). The solid line is for a sample in the absence of fatty acid; the dotted line is for a sample containing 30 μM oleic acid. The exitation wavelength was 280 nm.

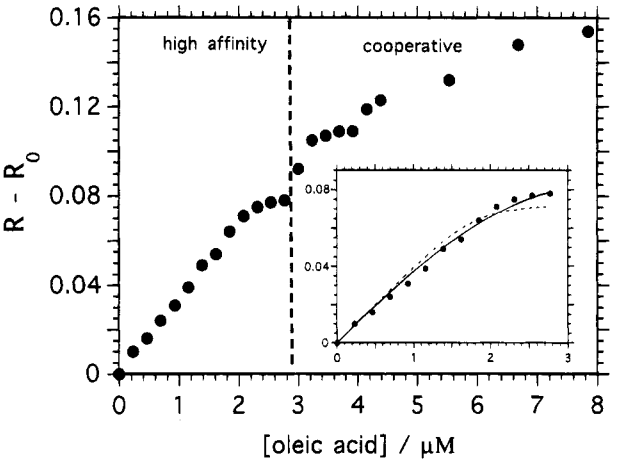

FIGURE 7: Blue shift ($R - R_0$) in the intensity ratio of the intrinsic fluorescence of LpL (0.45 μM) as a function of added oleic acid. The intensity ratio is the fluorescence intensity at 318 nm relative to that at 342 nm. The shift in the low concentration regime corresponds to high-affinity binding, whereas the shift after the reproducible breakpoint is due to cooperative binding of oleic acid (see text for details). Inset: Best fit to eq 7 for data obtained in the high-affinity regime by assuming $p = 4$ and $K_d = 0.042$ μM (– – –) or $p = 5$ and $K_d = 0.27$ μM (—).

addition of oleic acid to 0.45 μM LpL. A break is observed in the binding curve at 2.7 μM oleic acid. This break point is reproducible and corresponds to the point at which the formation of micellar-like aggregates is expected to begin (Figure 3). The increase in the intensity ratio observed at higher oleate concentrations probably represents the formation of large molecular weight fatty acid–LpL complexes, the spectral shift being caused by the more hydrophobic milieu created around tryptophan residues on the LpL as a result of the formation of the micellar-like complexes. The formation of the fatty acid–LpL complexes is a highly cooperative event, as is micelle formation in general, and we will refer to this part of the binding isotherm as the cooperative binding region. We examine first the spectral shift representing high-affinity binding.

Analysis of the Spectral Shift in the High-Affinity Region. We derive an expression describing the shift in the intensity ratio as a function of the total concentration of added fatty

acid. We assume that the sites are equivalent and independent and have an average dissociation constant described by the following equilibrium binding expression:

$$K_d = [FA]_{free}(p[LpL]_{tot} - [FA]_{bound})/[FA]_{bound} \quad (4)$$

Equation 4 may be rearranged to

$$[FA]_{bound}^2 - [FA]_{bound}([FA]_{tot} + p[LpL]_{tot} + K_d) + [FA]_{tot}p[LpL]_{tot} = 0 \quad (5)$$

In addition,

$$R - R_0 = ([FA]_{bound}/p[LpL]_{tot})(R_{max} - R_0) \quad (6)$$

where $(R_0 - R_{max})$ is the change in intensity ratio corresponding to full saturation of the high-affinity sites. Equations 5 and 6 may be combined to give the following expression, which describes the change in the fluorescence ratio as a function of the total concentration of added fatty acid:

$$R - R_0 = [([FA]_{tot} + p[LpL]_{tot} + K_d - (([FA]_{tot} + p[LpL]_{tot} + K_d)^2 - 4[FA]_{tot}p[LpL]_{tot})^{1/2})/2p[LpL]_{tot}](R_{max} - R_0) \quad (7)$$

K_d, p, and $(R_{max} - R_0)$ may be evaluated by using a nonlinear regression fit of eq 7 to the high-affinity data in Figure 7.

The presence of the cooperative binding region complicates this analysis. Binding may not be tight enough that full saturation of the high-affinity sites is reached before the cooperative binding phase sets in. In this situation, the determination of R_{max} becomes uncertain, leading to errors in the estimation of the binding parameters by use of eq 7. The best fit to the first 13 data points in Figure 7 was for five binding sites, with a K_d of 5×10^{-9} M. Such a low dissociation constant is unlikely. For comparison, bovine serum albumin (BSA) has two or three high-affinity binding sites ($K_d = 10^{-7}$ M) for long chain fatty acids; application of a multiple binding model suggests that the site with the strongest affinity has a K_d of about 6×10^{-9} M for oleic acid [Spector (1986) and references therein].

An alternative analysis of the data obtained in the high-affinity region of Figure 7 may be obtained if we use the information obtained from titration of the apparent CMC. This analysis shows that the minimum number of binding sites is four. Application of eq 2 allows the calculation of K_d values corresponding to four or more binding sites. The values of p and K_d may thereafter be inserted into eq 7 and fit to the spectral shift data obtained in the high-affinity region. As seen in the inset of Figure 7, a better fit is obtained for $p = 5$ and $Kd = 0.27$ μM than for $p = 4$ and $Kd = 0.042$ μM. However, acceptable fits are also obtained for higher values of p and the corresponding K_d values (not shown). It thus appears that the number of binding sites should equal at least five, but the uncertain data in the vincinity of the cooperative region make it difficult to discriminate further with respect to the number of possible sites.

Analysis of the blue shift is less difficult for fatty acid soaps that form crystals above their solubility limits. As the solubility limit is reached and phase separation takes place, the concentration of monomer fatty acid remains constant and no further binding to high-affinity sites is expected. Furthermore, the formation of the fatty acid–LpL complexes requires self-assembly of the fatty acid into micellar-like structures. Thus, no cooperative binding leading to the formation of complexes is expected for fatty acids that form crystals above their solubility limits.

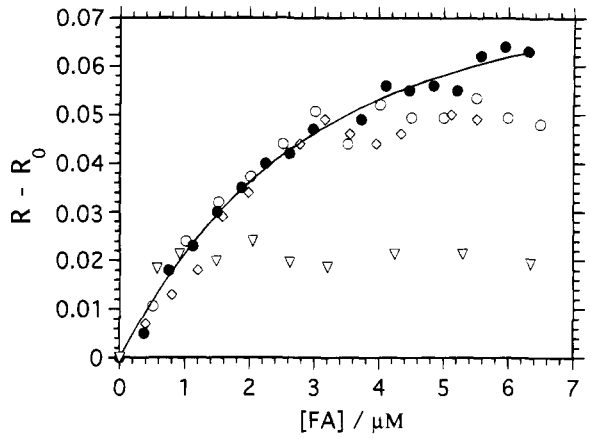

FIGURE 8: Shift in intensity ratio $(R - R_0)$ as a function of added petroselinic (●), petroselaidic (○), elaidic (◇), and stearic acids (▽). The solid line represents the best fit of eq 7 to the data obtained for petroselinic acid. The LpL concentration was 0.45 μM. Note the absence of a breakpoint, which in the case of oleic acid indicates (Figure 7) the onset of the cooperative phase of binding.

Petroselinic and petroselaidic acids are cis and trans monounsaturated fatty acids, respectively, with the double bond located at the Δ^6-position in the 18-carbon acyl chains. Elaidic acid is the Δ^9 trans isomer of oleic acid. Like stearic acid, petroselinic, petroselaidic, and elaidic acids have chain melting temperatures higher than that for oleic acid, and their sodium soaps are not expected to form micelles at room temperature. When the concentration of the sodium salts of these fatty acids is increased above the solubility limit, with the consequent formation of soap crystals, the spectral shift remains constant. Figure 8 shows the shift in intensity ratio as a function of fatty acid concentration for these fatty acids. The blue shift corresponding to high-affinity binding is observed at low ligand concentrations, but the region of cooperative binding at high concentrations is absent. For stearic acid, which has the lowest solubility, constant shift ratios are reached at very low total concentrations of ligand, whereas for petroselaidic, petroselinic, and elaidic acids the binding continues closer to the point of saturation of the high-affinity sites.

Data for the high-affinity binding of petroselinic acid were analyzed according to eq 7. When the three parameters, p, K_d, and R_{max}, were allowed to float, the best fit provided $p = 3.5$ and $K_d = 1.8$ μM. However, the number of binding sites must be an integer, and the data were therefore reanalyzed with p fixed at 4, 5, and 6. Reasonable fits, with values for K_d of 1.6, 1.1, and 0.73 μM, respectively, were obtained, and the corresponding Scatchard plots were linear (not shown). However, for $p > 6$, the best fit using eq 7 significantly deviates from the data points, particularly at low ligand concentrations (Figure 9). The blue shift obtained with the trans unsaturated acids could not be followed to high enough concentrations to allow accurate analysis of the data using eq 7.

Analysis of the Spectral Shift in the Cooperative Region. The binding of oleic acid in the cooperative binding region was investigated further in a separate experiment. The blue shift continues until the fatty acid/LpL molar ratio reaches

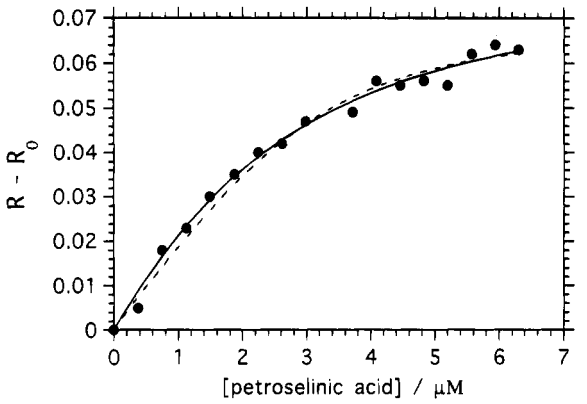

FIGURE 9: Best fit to eq 7 of the data obtained for the high-affinity binding of petroselinic acid to LpL: —, assuming four binding sites; – –, assuming seven binding sites.

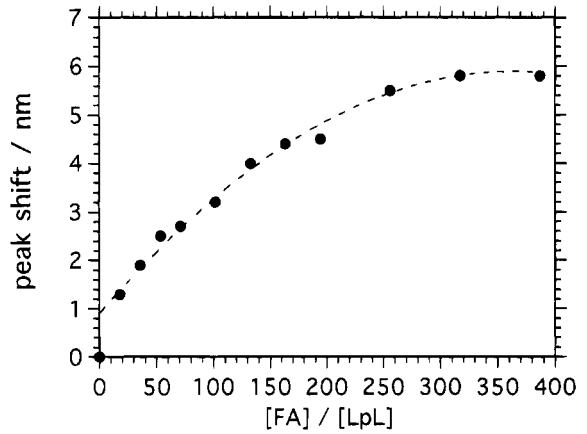

FIGURE 10: Shift in the emission maximum as a function of added oleic acid for a sample containing 0.15 μM LpL. All data points correspond to concentrations of oleic acid in the cooperative binding region (see Figure 7).

values in the range of 260−310 (Figure 10). In this region, the proportion of fatty acids adsorbed to the glass walls of the cuvette or at the air/water interface may be neglected, and the data obtained close to the saturation limit indicate complexes containing 1.5−1.8 g of fatty acid/g of LpL or a molar ratio of oleic acid to LpL of close to 300.

The binding isotherm in Figure 10 does not show the sigmoidal shape characteristic for cooperative binding. However, a sigmoidal curve can be expected only if the spectral shift over the whole region is directly proportional to the number of fatty acid molecules associated with the fatty acid−LpL complex. From Figure 10, it appears as though progressively smaller shift is induced as the size of the complex increases.

To summarize, for fatty acids that form micellar structures, the binding of fatty acids to LpL occurs in two stages, as revealed by the shift in the emission maximum. Relatively tight binding occurs at fatty acid concentrations below the apparent CMC. At a reproducible break point, a second and more pronounced blue shift is observed, corresponding to the formation of large complexes with a fatty acid−LpL ratio of close to 300. The biphasic nature of the blue shift was not observed in the case of a special class of fatty acids, namely, those whose sodium soaps have critical micellar temperatures above the current temperature range. For example, elaidic acid shows the spectral shift due to tight binding below the solubility limit, but the second phase representing cooperative binding is absent (Figure 8).

DISCUSSION

The solution behavior of fatty acids and their corresponding fatty acid salts is complex and depends on a number of environmental parameters, such as pH, temperature, and the type and concentration of the counterion, as well as on the chain length, saturation, and concentration of the fatty acid itself [Small (1986) and references therein]. Un-ionized long chain fatty acids have very low solubilities in water. On the other hand, fatty acid salts or soaps often have a relatively high solubility. Whereas fatty acids crystallize and precipitate at concentrations above their solubility limits, the apparent solubility of soaps may be further enhanced by the formation of micelles. However, micelle formation requires temperatures above the critical micellar temperature, which for fatty acids is closely related to the chain melting temperature. Below this temperature, which varies with the length, saturation, and conformation of the hydrocarbon chain, soap crystals form as the solubility limit is exceeded (Small, 1986). The concentration at which amphiphilic molecules start to aggregate into micelles is termed the critical micellar concentration. This concentration is also approximately equal to the maximum concentration of monomers in solution (Tanford, 1980). For sodium soaps of fatty acids, the micelles formed at concentrations just above the CMC are believed to be nearly spherical in shape and fairly monodisperse in size, whereas at higher concentrations, the micelles grow into elongated cylindrical structures (Reiss-Husson & Luzzati, 1966).

Many surfactants form stable complexes with proteins. These interactions have been studied extensively since they are of importance in a variety of biological, pharmaceutical, and industrial systems. More generally, factors controlling surfactant−polymer interactions and, in particular, surfactant−polyelectrolyte interactions have received particular attention. In this context, proteins may be regarded as amphoteric polyelectrolytes, and many of the characteristics of surfactant−polyelectrolyte systems are apparent in surfactant−protein systems. However, because proteins exhibit secondary and tertiary structure, the interaction between surfactants and proteins is more complex. In addition, the type of interaction and the complexes formed appear to vary somewhat, depending on the nature and structure of the protein. For example, the interaction between a surfactant and a soluble protein differs from that between a surfactant and an insoluble protein in a number of ways [Ananthapadmanabhan (1993) and references therein]. The binding of surfactants to proteins is also dependent upon the nature of the hydrophilic group on the surfactant. Thus, there can be significant differences between the binding of anionic, cationic, and nonionic surfactants to the same protein. However, some generalizations can be made. As with surfactant-polymer systems (Lindman & Thalberg, 1993), the binding of surfactants to proteins is nonspecific and highly cooperative in nature, and both the onset and saturation of the binding take place at well-defined concentrations of surfactant. The main driving force for nonspecific cooperative binding is the hydrophobic interaction between the chains of the surfactant and the nonpolar residues on the protein.

Much attention has been directed toward the complexes formed between soluble proteins and the anionic surfactant, sodium dodecyl sulfate (SDS). A number of different models have been suggested, including the necklace (Shirahama et

al., 1974), rodlike (Reynolds & Tanford, 1970), and flexible helix models (Lundahl et al., 1986). A protein-decorated micelle structure has also been proposed (Ibel et al., 1990). Many seemingly contradictory results have been reported, and no model satisfactorily accounts for all of the data presented. It is not unreasonable to assume that several different structures may be formed, depending on the size and nature of the interacting proteins and surfactants. However, it is clear that the surfactant−protein complexes possess micelle-like characteristics and that their structure is linked to, and is dependent upon, the self-aggregating properties of the surfactant.

In addition to nonspecific cooperative binding, many surfactants also bind to specific high-affinity sites on the proteins. This high-energy binding may involve both electrostatic and hydrophobic interactions and takes place at lower concentrations than those at which cooperative binding occurs. For a given surfactant, specific binding and therefore the initial part of the binding isotherm may vary between individual proteins, whereas at higher concentrations cooperative binding and the saturation limit appear to be relatively independent of the protein.

SDS is known to stabilize lipoprotein lipase in solution (Baginsky & Brown, 1977), presumably due to the formation of SDS−LpL complexes. Oleic acid, which in this context may be regarded as an anionic surfactant, also stabilizes LpL, and it has been suggested that it forms stable complexes with the protein (Bengtsson & Olivecrona, 1980). In addition, it has been presumed that LpL possesses specific high-affinity binding sites for oleic acid because of its ability to inhibit enzyme activity. However, no direct measurements of fatty acid binding have been reported. In this study, we have examined the binding of fatty acids to LpL in both the specific and cooperative binding regimes, making use of techniques that distinguish between the two processes.

The LpL-induced increase in the apparent CMC provides a means of detecting the specific binding of those fatty acids that have relatively low critical micelle temperatures and that therefore form micellar structures at room temperature. Using these procedures, the protein appears to possess a minimum of four sites for oleic acid, and the introduction of an additional double bond decreases the binding affinity by about 200-fold. The blue shift accompanying the binding of fatty acids can also be used to quantitate the binding equilibrium if the cooperative phase of the binding is taken into consideration. This may be achieved by choosing fatty acids that do not form micelles at room temperature, such as those with relatively high critical micelle temperatures. For these fatty acids, the formation of crystals takes place as the monomeric fatty acid concentration reaches the solubility limit. No micellar-like fatty acid−LpL complexes are formed, and as a result, only the first phase, corresponding to the binding of fatty acids to high-affinity sites, is observed for these fatty acids.

The decrease in the aqueous monomeric concentration at which the self-association of oleic acid takes place in the presence of LpL, compared to the CMC obtained in pure buffer (1.0 μM compared to 0.86 μM), indicates that the LpL−oleic acid micellar complexes have a lower CMC than pure oleic acid. This observation is not unique for the oleic acid−LpL system. The concentration needed for self-association of various surfactants has been shown to decrease in the presence of polymers and polyelectrolytes (Lindman & Thalberg, 1993).

The question of the structure of the fatty acid−LpL complexes is not addressed in the present study. However, as LpL does not lose activity, even after prolonged incubation with high concentrations of either SDS (Baginsky & Brown, 1977) or oleate (Olivecrona & Bengtsson-Olivecrona , 1980), these surfactants do not induce denaturation of the protein. LpL contains 10 disulfide bridges (Wang et al., 1990), which probably assist in stabilizing the protein. The absence of irreversible denaturation seems to rule out the necklace model (Shirahama et al., 1974), which requires the protein to unfold more or less completely. For the same reason, the flexible helix model (Lundahl et al.,. 1986) seems unlikely. A prolate ellipsoid built up by surfactant and protein, as described in the rodlike model (Renyolds & Tanford, 1970), remains a plausible model of the LpL−fatty acid complex. Other alternatives in which the protein remains intact, or is only partly unfolded, are also possible. The actual structure of the complexes remains to be thoroughly investigated.

In the experiments described, aggregation and subsequent precipitation of the enzyme were prevented by the inclusion of 1.5 M NaCl in the buffer. High salt concentrations may affect the binding in both the high-affinity region and the cooperative region. High concentrations of electrolyte decrease the net repulsive force between the negatively charged headgroups on the fatty acid, thereby positively affecting the binding in the cooperative region. On the other hand, in the high-affinity region, attraction between the negatively charged fatty acids and positively charged groups on the protein may be of importance, and the screening effect brought about by the addition of salt may thus decrease the binding affinity in this region. LpL does not dissociate from dimers to monomers at high ionic strength (Osborne et al., 1985). Thus, the fatty acid binding sites are unlikely to be at the interface between two monomer units in the dimer. Nevertheless, the binding of fatty acids under more physiological conditions of ionic strength and in the presence of heparin needs to be determined.

At sub-micromolar concentrations, the adsorption of fatty acids to the glass walls of the sample cell becomes important and must be taken into account in the experimental design and data analysis. In addition, fatty acids may adsorb at the air/water interface of the fluid surface in the sample cell. Because of adsorption, the point of self-association occurs at a concentration somewhat higher than the true value. Thus, the value for $[\text{oleate}]_{\text{free}}$ obtained from a plot such as Figure 3 corresponds to the free monomer concentration plus the amount of fatty acid adsorbed at the liquid/air interface and adsorbed to the glass walls. K_d values calculated using eq 2 should be corrected to lower values. Moreover, the error introduced by adsorption may vary with the hydrophobicity of the fatty acid. Linoleate, which is considerably more hydrophilic than oleate, may, for example, be expected to adsorb less than oleate. Differences in the adsorption of fatty acids to the glass walls and/or the air/water interface do not explain the observed difference in binding affinity between oleate and linoleate.

The relatively low dissociation constants found in the present study suggest that specific binding of fatty acids to LpL may be important in situations where fatty acids are produced at rates higher than their rate of absorption by underlying tissue. In most binding studies, as well as activity assays, it has generally been assumed that BSA possesses six or seven binding sites with higher affinities for fatty acids than any potential binding site on LpL. The two or three

sites on BSA with highest affinities for fatty acids have dissociation constants of about 10^{-7} M, whereas the remaining three to five sites have K_d values in the 10^{-6}–10^{-5} M range (Spector, 1986). Our results indicate that the high-affinity sites on LpL have comparable, or even higher, affinities for fatty acids than at least the intermediate sites on BSA. Thus, even in the presence of BSA, low concentrations of fatty acids may remain bound to the high-affinity sites on LpL and perhaps modulate the hydrolytic activity of the enzyme.

Studies of the kinetics of LpL indicate that fatty acids act as competitive inhibitors of lipolysis. It is therefore likely that at least some of the high-affinity binding sites detected in the present study involve the binding of fatty acids at or near the active site in the N-terminal domain of the enzyme (Hadvary et al., 1991). However, it remains to be determined whether high-affinity sites for fatty acids overlap with the putative heparin binding site in the C-terminal domain (Enerback et al., 1987) or with the binding site for apolipoprotein C-II, the cofactor that significantly enhances the activity of LpL.

The results obtained for oleic acid in the present study show that fatty acid–LpL complexes may form when the concentration of free fatty acids is high. The formation of fatty acid–LpL complexes could be involved in both the fatty acid-mediated release of heparin-bound LpL and the inhibition of activity when LpL acts on triglycerides in micelles, bilayers, or emulsions. This hypothesis could, however, be checked experimentally. If the formation of fatty acid–LpL complexes is the major reason for the release of heparin-bound LpL and/or the observed inhibition of hydrolytic activity, these effects should not be observed under conditions where the fatty acids do not bind cooperatively to LpL. To our knowledge, all studies published to date have been concerned with the effects of oleic acid (Bengtsson & Olivecrona, 1980; Saxena et al., 1989) or linoleic acid (Petterson et al., 1990), both of which form micellar-like complexes with LpL. Similar studies based on the effects of fatty acids that do not bind cooperatively in the current temperature range, for example, stearic acid elaidic acid, should help resolve whether complex formation or high-affinity binding is the main reason for the observed product inhibition.

CONCLUSIONS

The results presented in this study show that fatty acids may interact with lipoprotein lipase in both a specific and a cooperative way. All of the fatty acids investigated showed high-affinity binding to LpL, and our results suggest four to six specific sites on each LpL monomer. The binding appears to be influenced somewhat by the conformation of the acyl chain of the fatty acid. An average K_d of about 10^{-6} M was obtained for petroselinic acid, whereas the data for oleic acid indicate a dissociation constant in the range of 10^{-7}–10^{-6} M. The data for linoleate indicate a lower affinity than those for both petroselinic and oleic acids.

In addition to high-affinity binding, oleic acid was found to bind cooperatively to LpL. Cooperative binding leads to the formation of large complexes consisting of 260–310 fatty acid monomers per LpL monomer. In the temperature range investigated, no cooperative binding was observed for fatty acids that formed crystals at their solubility limit rather than micelles (stearic, elaidic, petroselaidic, and petroselinic acids).

ACKNOWLEDGMENT

We thank Professor T. Olivecrona for supplying an LpL sample for a purification standard.

REFERENCES

Ananthapadmanabhan, K. P. (1993) in *Interactions of Surfactants with Polymers and Proteins* (Goddard, E. D., & Ananthapadmanabhan, K. P., Eds.) CRC Press, Boca Raton, FL.

Baginsky, M. L., & Brown, W. V. (1977) *J. Lipid Res. 18,* 423–437.

Bengtsson, G., & Olivecrona, T. (1979) *FEBS Lett. 106,* 345–348.

Bengtsson, G., & Olivecrona, T. (1980) *Eur. J. Biochem. 106,* 557–562.

Enerback, S., Semb, H., Bengtsson-Olivecrona, G., Carlsson, P., Hermansson, M.-L., Olivecrona, T., & Bjursell, G. (1987) *Gene 58,* 1–12.

Hadvary, P., Sidler, W., Meister, W., Vetter, W., & Wolfer, H. (1991) J. *Biol. Chem. 266,* 2021–2027.

Ibel, K., May, R. P., Kirschner, K., Szadkowski, H., Mascher, E., & Lundahl, P. (1990) *Eur. J. Biochem. 190,* 311–318.

Lindman, B., & Thalberg, K. (1993) in *Interactions of Surfactants with Polymers and Proteins* (Goddard, E. D., & Ananthapadmanabhan, K. P., Eds.) CRC Press, Boca Raton, FL.

Lundahl, P., Greijier, E., Sandberg, M., Cardell, S., & Eriksson, K. O. (1986) *Biochim. Biophys. Acta 873,* 20.

McLean, L. R., & Jackson, R. L. (1985) *Biochemistry 24,* 4196–4207.

Olivecrona, T., & Bengtsson-Olivecrona, G. (1985) in *Atheroma and Thrombosis* (Kakkar, V. V., Ed.) pp 250–256, Pitman, London.

Osborne, J. C., Bengtsson-Olivecrona, G., Lee, N. S., & Olivecrona, T. (1985) *Biochemistry 24,* 5606–5611.

Peterson, J., Bihain, B. E., Bengtsson-Olivecrona, G., Deckelbaum, R. J., Carpentier, Y. A., & Olivecrona, T. (1990) *Proc. Natl. Acad. Sci. U.S.A. 87,* 909–913.

Posner, I., & DeSanctis, J. (1987) *Biochemistry 26,* 3711–3717.

Reiss-Husson, F., & Luzzati, V. (1966) *J. Colloid Interface Sci. 21,* 534–544.

Reynolds, J. A., & Tanford, C. (1970) *Proc. Natl. Acad. Sci. U.S.A. 66,* 1002–1007.

Richieri, G. V., Ogata, R. T., & Kleinfeld, A. M. (1992) *J. Biol. Chem. 267,* 23495–23501.

Saxena, U., Witte, L. D., & Goldberg, I. J. (1989) *J. Biol. Chem. 264,* 4349–4355.

Shirhama, K., Tsujii, K., & Takagi, T. (1974) *J. Biochem. (Tokyo) 75,* 309–319.

Simpson, B. R., Ashbrook, J. D., Santos, E. C., & Spector, A. A. (1974) *J. Lipid Res. 15,* 415–423.

Small, D. M. (1986) in *The Physical Chemistry of Lipids, Handbook of Lipid Research 4* (Hanahan, D. J., Ed.) Plenum Press, New York.

Spector, A. A. (1986) *Methods Enzymol. 128,* 320–339.

Tanford, C. (1980) in *The Hydrophobic Effect,* John Wiley & Sons, New York.

van Tilbeurg, H., Egloff, M.-P., Martinez, C., Rugani, N., Verger, R., & Cambillau, C. (1993) *Nature 362,* 814–820.

van Tilbeurg, H., Roussel, A., Lalouel, J.-M., & Cambillau, C. (1994) *J. Biol. Chem. 269,* 4626–4633.

Wang, C., Hartsuck, J., & McConathy, W. J. (1992) *Biochim. Biophys. Acta 1123,* 1–17.